Plant Physiology and Biochemistry 143 (2019) 1–10

Contents lists available at ScienceDirect

Plant Physiology and Biochemistry

journal homepage: www.elsevier.com/locate/plaphy

Research article

Three *NPF* genes in *Arabidopsis* are necessary for normal nitrogen cycling under low nitrogen stress

Benjamin A. Babst[a,b,4,*], Fei Gao[a,b,1], Lucia M. Acosta-Gamboa[c], Abhijit Karve[a,2], Michael J. Schueller[a,3], Argelia Lorence[c,d]

[a] Biosciences Department, Brookhaven National Laboratory, Upton, NY, 11973, USA
[b] Arkansas Forest Resources Center, Division of Agriculture, University of Arkansas, Monticello, AR, 71656, USA
[c] Phenomics Facility, Arkansas Biosciences Institute, Arkansas State University, Jonesboro, AR, 72467, USA
[d] Department of Chemistry and Physics, Arkansas State University, P.O. Box 419, State University, AR, 72467, USA

ARTICLE INFO

Keywords:
Nitrogen transport
Organic nitrogen cycling
Nitrate/peptide transporter family
Nitrogen stress
Source-sink interactions

ABSTRACT

Internal nitrogen (N) cycling is crucial to N use efficiency. For example, N may be remobilized from older, shaded leaves to young leaves near the apex that receive more direct sunlight, where the N can be used more effectively for photosynthesis. Yet our understanding of the mechanisms and regulation of N transport is limited. To identify relevant transporters in *Arabidopsis*, fifteen transporter knockout mutants were screened for defects in leaf N export using nitrogen-13 (^{13}N) administered as $^{13}NH_3$ gas to leaves. We found that three nitrate/peptide transporter family (*NPF*) genes were necessary for normal leaf N export under low N but not adequate soil N availability, including *AtNPF7.1*, which has not been previously characterized. High-throughput phenotyping revealed altered leaf area and chlorophyll fluorescence relative to wild-type plants. High *AtNPF7.1* expression in flowers and large flower stalks of *Atnpf7.1* mutants in low N suggests that *AtNPF7.1* influences leaf N export via sink-to-source feedback, perhaps via a role in sensing plant internal N-status. We also identified previously unreported phenotypes for the mutants of the other two NPF transporters that indicate possible roles in N sensing networks.

1. Introduction

Crop productivity needs to increase while using less arable land in the near future to meet the growing needs of our growing global population for food, fiber, and wood. Nitrogen (N) is often the most limiting nutrient for terrestrial plants, since plants rely heavily on biological N fixation to replenish N lost from the soil by leaching, runoff, and as gases from denitrification, making the stress associated with N deficiency commonplace. Simply increasing fertilization is not a sustainable solution in the long-term (Ferrieri et al., 2018). Investigating plant N allocation in order to identify strategies to improve N use efficiency (NUE) is a promising approach. Symptoms of N-stress include yellowing of leaves, smaller leaf area, and reduced photosynthetic rates, which result in reduced growth rates. Nitrogen uptake is well studied, but optimal distribution of N within the plant is necessary in order to maximize growth (Tegeder and Masclaux-Daubresse, 2018). Not only does N need to be transported from roots to leaves, but N must also be re-distributed amongst organs at several phases of development (Babst and Coleman, 2018; Diaz et al., 2008; Havé et al., 2017; Taylor et al., 2010).

A major knowledge gap is our limited understanding of the mechanisms and specific genes that drive N transport and how N transport is regulated, especially N export from leaves (Babst and Coleman, 2018; Tegeder and Masclaux-Daubresse, 2018). Nitrogen export from leaves is crucial to retain and recycle N within the plant, and is also important to supply normal sink N needs during the growing season, since most N assimilation occurs in leaves. Export of N from leaves is especially important during N-stress to move N from old partially shaded leaves to the youngest, best lit leaves.

Although the phloem is thought to be the main vascular pipeline for

* Corresponding author. Arkansas Forest Resources Center, Division of Agriculture, University of ARkansas, Monticello, AR, 71656, USA.
E-mail address: babst@uamont.edu (B.A. Babst).
[1] Present address: Division of Plant Sciences, University of Missouri, Columbia, MO, 65211, USA.
[2] Present address: Purdue Research Foundation, West Lafayette, IN, 47906, USA.
[3] Present address: Missouri Research Reactor Center and Department of Chemistry, University of Missouri, Columbia, MO, 65211, USA.
[4] Present address: College of Forestry, Agriculture & Natural Resources, University of Arkansas at Monticello, Monticello, AR, 71656, USA.

https://doi.org/10.1016/j.plaphy.2019.08.014
Received 23 May 2019; Received in revised form 10 August 2019; Accepted 19 August 2019
Available online 20 August 2019

carbon (C) and N transport out of leaves, a recent study indicates that C and N transport are driven by independent mechanisms (Gomez et al., 2010). Since vascular transport is largely dependent on bulk flow of fluids through an open pipeline (i.e., phloem), these differences between C and N transport are likely due to differences in the loading and unloading of specific biological molecules into and out of the phloem by transporters that move specific molecules across cell membranes. Few N specific transporters have been identified in the phloem (e.g., NRT1.7, AAP2, and AAP8) (Fan et al., 2009; Santiago and Tegeder, 2016; Zhang et al., 2010). Yet, there are large gene families with similar coding sequences that likely play other important roles in regulating N distribution throughout the plant (e.g., over 50 members of NPF, nitrate transporter/peptide transporter family; 7 members of NRT2, nitrate transporter 2 family; 8 members of AAP, amino acid permease family, in *Arabidopsis*) (Léran et al., 2014; Santiago and Tegeder, 2016), and many of the transporters of organic N (e.g., amino acids) are yet to be identified (Tegeder, 2012).

The N transporters that are necessary for normal N export from leaves could have one of several possible biological roles in the pathway to the phloem. First, the N that is exported from leaves may be metabolized before being exported. Since various aspects of N metabolism may occur in different sub-cellular compartments (e.g., cytosol, chloroplast, mitochondria), N transport across organelle membranes might be essential for normal N export. Second, sugars (i.e., C) move through a series of cell types en route to the phloem (e.g., mesophyll, bundle sheath, parenchyma, and apoplast), and N transporters may be important for moving N along this physical pathway within tissues. Third, N transporters may act directly in loading N into the sieve elements or companion cells of the phloem.

Study of N export from leaves on a short time-frame is challenging. Application of nitrogen-15 (^{15}N) stable isotope tracers to leaves is logistically challenging and must be at high enough concentration to detect above natural abundance ^{15}N. The ^{15}N itself may elicit a response, and alter the system in the process of trying to study it. The positron-emitting isotope nitrogen-13 (^{13}N), the only useful radioactive isotope of N, has been used to probe leaf N metabolism without perturbing the system (Hanik et al., 2010). Inorganic N is normally assimilated into organic N via the glutamine synthetase-glutamate synthase (GS-GOGAT) cycle. By supplying ^{13}N as $^{13}NH_3$ gas to intact leaves at concentrations below the natural abundance of NH_3 in plant tissues, ^{13}N is assimilated into normal N metabolism via the GS-GOGAT cycle. Thus, $^{13}NH_3$ can be used to probe specific N biochemical pathways and/or N transport from leaves.

Taking a systems biology perspective, the objective of this study was to identify genes that are directly responsible for N transport during remobilization, or that regulate the N transport system. The availability of mutants and massive global gene expression data sets for the reference plant *Arabidopsis thaliana* were leveraged to generate co-expression networks, which were used to winnow the list of candidate N transporter encoding genes from > 1000 to fewer than 50 (He et al., 2016). Here we report the results of screening 15 of these mutants, by which we identified 3 *AtNPF* mutant lines that exhibited altered N transport in ^{13}N radiotracer transport assays. Two of the AtNPFs were previously characterized as nitrate transporters in *Arabidopsis*, and one (*AtNPF7.1*) has not been investigated previously. We further examined the three mutant lines using a high-throughput phenotyping (HTP) system to help characterize the *in vivo* role of the three AtNPFs.

2. Material and methods

2.1. Plant materials and growth conditions

Arabidopsis Columbia wild-type (Col-0) and T-DNA mutants (*Atnpf4.6*, *Atnpf2.12*, *Atnpf2.13*, *Atnpf7.1*) were obtained from the Arabidopsis Biological Resource Center (ABRC, Columbus, OH, USA). *Arabidopsis* seeds were germinated in ½ MS medium (Murashige and Skoog, 1962) for 10–12 days. For ^{13}N experiments, seedlings were transplanted into potting soil (Professional Growing Mix, Sungro®, Agawam, MA) in plastic pots (8 x 8 × 7 cm). The adequate N treatment plants were grown on potting mix for the duration of the experiment. Since we were unable to achieve a low N treatment in a peat-based potting mix, for low N treatment, the seedlings were grown on potting mix for 15–18 days and transplanted to Profile Greens Grade Soil Amendment. *Arabidopsis* plants were grown in a plant growth chamber (MTR30, Conviron, Canada) under a short-day photoperiod (10-h light, 24 °C daytime, 22 °C dark, 65% humidity) for total of 6–8 weeks and then used for ^{13}N experiments. Light was provided by fluorescent tubes (F40PL/AQ/ECO 49893 40Watt T12, GE) at a photon flux density of ~190–210 μmol m^{-2} sec^{-1} measured at the top of the pots.

For high-throughput phenotyping, *Arabidopsis* plants were grown as above, except all seedlings were transplanted into Profile Greens Grade Soil Amendment (PROFILE Products LLC, Buffalo Grove, IL) with one teaspoon (4.9 ml) of potting soil packed into the center to help with the initial survival of transplanting. Each genotype/treatment were grown in 85 × 73 mm Quick Pot 15 RW trays (HerkuPlast Kubern GmbH) in a controlled-environment chamber (Conviron) at 22 ± 1 °C, 65 ± 5% RH, and 160–200 μmol m^{-2} s^{-1} PAR light intensity. "Adequate" and "low" N nutrient solutions were added once per week by bottom watering to appropriate treatment groups, and deionized water was added once per week in between fertilizer additions. Pilot studies using different N concentrations were conducted to determine what N additions to Profile Greens medium would allow growth similar to plants in a standard peat-based potting mix, and what level of N addition would serve as a low N treatment. Nutrient solutions were made by mixing Murashige & Skoog with Gamborg's vitamins (MSP06, Caisson Laboratories, Smithfield, UT) and Murashige & Skoog without Nitrates (MSP07, Caisson Labs) to achieve ½ MS with either 1/10th the amount of N in normal ½ MS (6 mM N, adequate N) or 1/50th (1.2 mM N, low N) in deionized H_2O.

2.2. Assay of N export from leaves using $^{13}NH_3$

Using intact plants, ^{13}N ($t_{1/2}$ = 9.97 min) was administered as $^{13}NH_3$ gas to individual leaves in leaf cuvettes (Gomez et al., 2010; Hanik et al., 2010). The ^{13}N was produced as $^{13}NO_3^-$ by the $^{16}O(p,\alpha)^{13}N$ nuclear transformation in a sealed water target using the 19 MeV TR19 cyclotron (EBCO, Richmond, BC, Canada) at Brookhaven National Laboratory (Ferrieri and Wolf, 1983; Straatman, 1977). The resulting aqueous $^{13}NO_3^-$ solution was heated in the presence of de-Varda's alloy and alkalinized with potassium hydroxide to reduce the $^{13}NO_3^-$ to $^{13}NH_3$ for isotope removal as gaseous $^{13}NH_3$. The $^{13}NH_3$ tracer was then administered with the stream of air to a single leaf on each plant at high specific activity using a leaf cuvette (Fig. 1). The highly sensitive detection and high specific activity of $^{13}NH_3$, which becomes $^{13}NH_4^+$ at cellular pH, allows feeding of the tracer at concentrations that are orders of magnitude below the natural abundance level of ammonium in leaf tissues, such that the ^{13}N is a true tracer utilized in metabolism and transported throughout the plant, without perturbing N homeostasis (Gomez et al., 2010; Hanik et al., 2010; Pankievicz et al., 2015).

Up to six *Arabidopsis* plants at one time were used for the $^{13}NH_3$ assay. At least 30 min before the $^{13}NH_3$ was delivered, a single large rosette leaf was selected as the load leaf (the 8th-10th leaf) and clamped into the cuvette with a pump attached to the outlet for the duration of the incubation to maintain airflow. Gaseous $^{13}NH_3$ was delivered into the cuvette for 15 min. After 45 min, each plant was dissected to 5 parts (6 if the plant was bolting): Rosette leaves (RsL); rosette stems (RsS); flower stalks (stem); petiole and the half of the load leaf not in the cuvette; the load zone, which is the part of the leaf in the cuvette; and the roots (profile greens were washed off with water). The radioactivity of each plant part was measured in a shielded gamma radiation well counter (Model 203, NATS Inc., Middletown, CT, USA; Scaler/

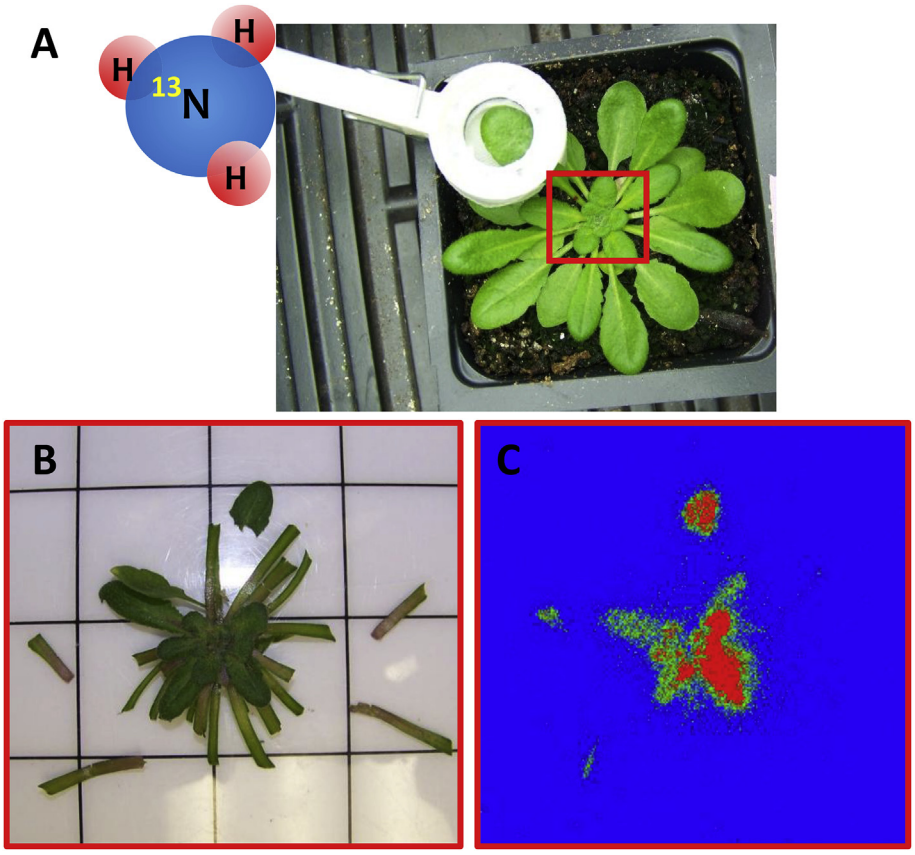

Fig. 1. Use of $^{13}NH_3$ as a tracer of N transport from a leaf to other parts of the plant. (A) Cuvette for delivery of $^{13}NH_3$ to a single leaf of *Arabidopsis* plants. **(B)** *Arabidopsis* rosette (from red box in ***A***, magnified) dissected 45 min after receiving $^{13}NH_3$ to one leaf to determine distribution of the ^{13}N. **(C)** Phosphor plate image showing distribution of radioactivity from ^{13}N in young leaves of the dissected plant in **(B)**. (For interpretation of the references to color in this figure legend, the reader is referred to the Web version of this article.)

Ratemeter Model 2200, Ludlum Measurements, Inc., Sweetwater, TX), calibrated using a NIST-calibrated source, and the time was recorded for decay correction. The plant tissues were dried in an oven at 70 °C for 2 days, and weighed.

To quantify how much ^{13}N had been assimilated in the leaf, a piece of the load zone was cut off and the radioactivity of the piece was measured. The leaf piece was ground in 1M KOH solution to convert any remaining $^{13}NH_4^+$ to the volatile form $^{13}NH_3$, and Ar gas was bubbled through the solution for 5, 10, 20min to 1hr to remove any $^{13}NH_3$. We found no reduction in decay-corrected radioactivity in the leaf tissue by the end of the 1 h incubation, indicating that all ^{13}N remaining in the leaf at the time of harvest had been assimilated by the plant.

2.3. ^{13}N calculations

To account for radioactive decay, which is highly predictable based on the half-life of the isotope, all radioactivity measurements were decay corrected to the time of $^{13}NH_3$ feeding to the plant. Radioactivity from the gamma well counter was converted to decays per minute (dpm) based on the calibration of the counter using a NIST calibrated radiation source, and then converted from dpm to MBq prior to decay correction. Partitioning of ^{13}N to each plant part was calculated using the radioactivity measured in the part divided by the total activity detected in the whole plant. The ^{13}N export was calculated as the combined radioactivity of RsS, stem, petiole, and roots, as a percentage of the total activity in the plant. To account for variation in the mass of plant tissues, partitioning was normalized to dry weight (^{13}N % partitioning divided by dry weight).

2.4. High-throughput phenotyping of Arabidopsis plants

Phenotyping was done with a Scanalyzer HTS high-throughput phenotyping system using the LemnaControl software (Lemnatec, Aachen, Germany) starting 4–7 days after transplanting. Images were acquired three times per week to monitor plants in the vegetative stage through the transition to the reproductive stage. The system has a robotic arm to capture images with visible (RGB), fluorescence (FLUO), and near infrared (NIR) cameras. We analyzed images for differences between N-treatments and genotypes in the rosette size, leaf shape and area, *in planta* chlorophyll fluorescence, and *in planta* water content. Image acquisition and analysis was done as previously described (Acosta-Gamboa et al., 2016). Phenotyping experiments were terminated when the flower stalks reached the cameras, affecting the focusing of the images, after which plant tissues were harvested for RT-qPCR analysis of gene expression. Each *Arabidopsis* plant was divided into young rosette leaves, old rosette leaves, rosette stem, flower stalk, cauline leaves, siliques, flowers, and roots for all four genotypes (Col-0, *Atnpf7.1*, *Atnpf4.6*, *Atnpf2.12*) and two treatments (adequate N; low N). For all tissues except flowers and siliques, each plant was treated as a separate replicate. Flowers and siliques were pooled from at least 2–3 plants in order to have enough tissue in each sample. The tissues were flash-frozen in liquid nitrogen, transported on dry-ice, and stored at −80 °C until used for RT-qPCR analysis.

2.5. Semi-quantitative RT-qPCR

To validate that mutants had reduced or eliminated expression of the genes of interest, we used semi-RT-qPCR. Total RNA was extracted from rosette leaves and flowers using a GeneJET Plant RNA Purification Kit (Thermo Scientific, MA, USA). RNA was treated with DNase I (Thermo Scientific, MA, USA), and the quantity and quality were assessed with a NanoDrop Microvolume Spectrophotometer (Thermo Scientific, MA). From 1 μg of total RNA, cDNA was synthesized using an oligo(dT)15 primer and Moloney murine leukemia virus (MMLV) reverse transcriptase (Thermo Scientific, MA) following the

Table 1
Average flower stalk (stem) length of plants used for ^{13}N partitioning measurements (bolting plants only).

plants	Average stem length (cm)
Col-0	4.76 ± 1.82
Atnpf4.6	6.63 ± 2.29
Atnpf2.12	2.44 ± 1.37
Atnpf7.1	8.62 ± 2.04
Atnpf2.13	9.04 ± 1.90

manufacturer's protocol. Equal amounts of cDNA were used as templates for each PCR reaction with Taq polymerase. The Actin2 gene (*At3g18780*) was used as a standard to normalize the transcript levels. Equal amounts of PCR product were separated on one electrophoresis gel, and brightness of the bands compared.

2.6. RT-qPCR

For RT-qPCR experiments, total RNA was extracted from the respective *Arabidopsis* tissues collected from the phenotyping experiments, and treated with DNase I, and 1 μg was used to synthesize cDNA, as described above. RT-qPCR was performed with a G8830A AriaMX Real-Time PCR System (Agilent Technologies, St. Clara, CA) following the manufacturer's manual, using SYBR Green QPCR Master Mix (Bio-Rad, CA). Each sample was run in triplicate in a 20 μl reaction volume. Thermal cycling conditions were as follows: 95 °C for 10 min, 65 cycles of 95 °C for 15 s, 60 °C for 30 s and 1 cycle of 95 °C for 1 min, 60 °C for 30 s and 95 °C for 30 s. The levels of transcripts were normalized using the *SAND* gene (At2g28390) mRNA levels as an internal standard. These experiments were performed at least twice with similar results. Primers used in qPCR experiments are listed in Suppl. Table 1.

2.7. Constructing transgenic Arabidopsis AtNPF7.1-promoter::GUS reporter lines

The *AtNPF7.1* promoter from *Arabidopsis* Col-0 (2015 bp upstream from the start codon) genomic DNA were cloned into the Gateway entry vector pDONR201 and sub-cloned into binary vector pYXT1 containing the GUS reporter gene. Primers used in cloning are listed in Table S1.

Transgenic *Arabidopsis* promoter–GUS reporter lines were generated by the floral dip method (Clough and Bent, 1998) using *Agrobacterium tumefaciens* strain GV3101. Transformants were screened on half-strength Murashige and Skoog medium (Caisson Labs) containing 50 mg ml^{-1} kanamycin (Sigma, St. Louis, MO). Single-locus homozygous transgenic lines expressing AtNPF7.1_{pro}:GUS were selected by scoring for the segregation of kanamycin resistance in the T_2 and T_3 generations.

2.8. Agrobacterium-mediated transient expression and confocal fluorescence microscopy

The yellow fluorescent protein (YFP) fusion binary constructs were transformed into *A. tumefaciens* strain C58C1 by the freeze-thaw method. Bacteria were cultured overnight, harvested by centrifugation and resuspended in 10 mM $MgCl_2$ with 100 mM acetosyringone (Fisher scientific, Lenexa, KS) and adjusted to an OD_{600} of 0.25–0.3. *Agrobacterium* was incubated for 2 h at room temperature and infiltrated into *N. benthamiana* leaves with a 1 ml needleless syringe. The *N. benthamiana* plants were placed under a 16 h light/8 h dark cycle at 25 °C. Tissues were collected 3 d after infiltration for confocal microscopy. Plant tissues were viewed directly under a Zeiss LSM 880 two-photon point-scanning confocal system mounted on an Axiovert 200M inverted microscope with a 40/1.2 C-Apochromat water immersion objective. Yellow fluorescent protein fluorescence was excited by a 514 nm argon laser. Sample fluorescence was detected using a 500–550 nm band-pass emission filter.

2.9. Histochemical GUS assays

To visualize GUS expression, whole plants or freshly excised tissues expressing AtNPF7.1_{pro}:GUS were soaked with substrate buffer (0.5 mM 5-bromo-4-chloro-3-indolyl glucuronide, 100 mM Tris, pH 7.0, 50 mM NaCl, 0.06% Triton X-100, 3 mM potassium ferricyanide) and were incubated at 37 °C for 16 h (Jefferson et al., 1987). Chlorophyll was cleared from stained tissue by incubating in 70% ethanol. Imaging was performed using a stereoscope and a digital camera.

2.10. Accession numbers

AtNPF4.6 (NRT1.2), At1g69850; AtNPF2.12 (NRT1.6), At1g27080; AtNPF2.13 (NRT1.7), At1g69870; AtNPF7.1, At5g19640.

2.11. T-DNA mutants

Atnpf4.6, SALK_072696C; *Atnpf2.12*, SALK_104042C; *Atnpf2.13*, SALK_022429C; *Atnpf7.1*, SALK_138950C (for other mutants screened, see Suppl. Table 2).

2.12. Statistical analysis

All data were analyzed with SAS v9.4 software (SAS Institute Inc., Cary, NC) using the PROC GLM ANOVA procedure. Where genotype or treatment effects were significant ($\alpha = 0.05$), the Dunnett post hoc multiple comparison was performed to compare each *Atnpf* mutant with the WT Col-0 genotype. Data were checked for ANOVA assumptions of normality and heteroscedasticity. Where the assumption of heteroscedasticity was not met, Welch's ANOVA, which does not assume equal variances, was used instead (McDonald, 2014). Where Welch's ANOVA indicated a statistically significant difference, Dunnett's T3 test was used for multiple comparisons (Dunnett, 1980).

3. Results

3.1. Identifying Arabidopsis leaf nitrogen export mutants using radioactive $^{13}NH_3$

Initially, we compiled mutants of nitrate transporter family genes that were expressed in senescing leaves (Breeze et al., 2011; Schmid et al., 2005). Subsequently, selection criteria evolved to include only genes that were differentially expressed during leaf senescence, and then narrowed further to genes that were co-expressed with genes that are known to be involved in N remobilization (Suppl. Table 2; Suppl. Fig. 1) (Breeze et al., 2011; He et al., 2016; Klepikova et al., 2016).

When a single fully expanded mature leaf with no visible signs of senescence on an *Arabidopsis* plant was exposed to $^{13}NH_3$, the ^{13}N that remained after 45 min could not be removed by alkaline sparging (see methods), indicating that the remaining ^{13}N had been assimilated in the leaf. A portion of the assimilated ^{13}N (0.5–1.5%) was exported from the leaf and could be detected in young leaves within 45 min (Fig. 1C). This export rate is much lower than typically found for carbon export (e.g., 30–45%) (Ferrieri et al., 2013), which was expected since proportionally more N is retained in leaves than C, but the export rate was sufficient to measure for comparisons between treatment groups. We tested fifteen N-related transporter mutants, and found that three mutants, *Atnpf4.6*, *Atnpf2.12* and *Atnpf7.1*, had significantly lower ^{13}N export from the rosette leaves on a sink tissue mass basis than wild-type (WT) plants under low soil N availability (Fig. 2A). On the contrary, the *Atnpf2.13* (previously *nrt1.7)* mutant had similar ^{13}N export from leaves as the WT. Since AtNPF2.13 is known to mediate export of inorganic NO_3^- from leaves (Fan et al., 2009), loss of AtNPF2.13 function was not expected to alter export of organic forms of N. The three mutants with

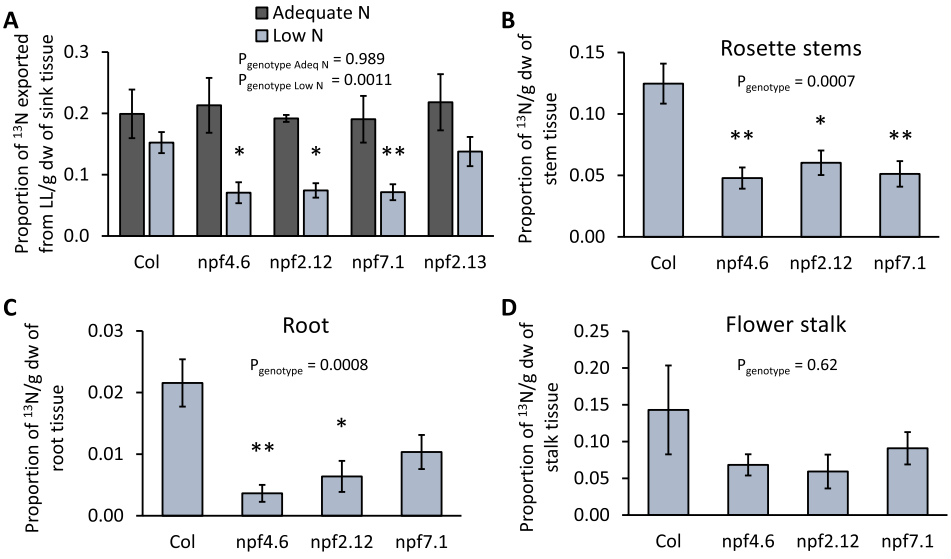

Fig. 2. Partitioning of ^{13}N was affected in *Atnpf4.6* (*nrt-1.2*), *Atnpf2.12* (*nrt-1.6*), and *Atnpf7.1* (*pot*) mutants under low N availability. (A) ^{13}N export was lower in several *Arabidopsis* mutants compared to WT under low N but not adequate N conditions. Bars indicate proportion of assimilated ^{13}N that was exported from the load leaf (LL) to sink tissues, normalized by sink tissue mass. Normalized partitioning of ^{13}N to **(B)** rosette stems, **(C)** roots, and **(D)** flower stalks only under low N conditions. Normalized partitioning was calculated as the proportion of total plant ^{13}N that was found in the sink tissue per unit mass of sink tissue. Error bars indicate standard error. P-values are for ANOVA, except that the p-value of roots is from a Welch's ANOVA since root ^{13}N data did not meet the assumption of heteroscedasticity. *P < 0.05; **P < 0.01.

reduced ^{13}N export from leaves, *Atnpf4.6*, *Atnpf2.12* and *Atnpf7.1*, were the focus of the remainder of this study. Semi-RT-qPCR verified that *AtNPF2.12* and *AtNPF7.1* expression was eliminated in their respective mutants, and *AtNPF4.6* transcript abundance was reduced in the *Atnpf4.6* mutant (Supp. Fig. 2).

The fact that reduced ^{13}N export in *Atnpf4.6*, *Atnpf2.12* and *Atnpf7.1* mutants was apparent only when soil N availability was low (Fig. 2A) suggests that *AtNPF4.6*, *AtNPF2.12* and *AtNPF7.*1 might be induced in low N conditions and serve some function in tolerance of low N stress. Sink-normalized N partitioning was reduced in rosette stems and roots (Fig. 2B–C). Although sink-normalized N partitioning appeared to be reduced in mutant flower stalks, the difference from WT was not statistically significant (Fig. 2D). During the transition from the vegetative to the reproductive stage, the rate of export of ^{13}N from leaves did not change, except in the *Atnpf2.12* mutant, where ^{13}N export from leaves decreased by about 50% (Fig. 3). Partitioning of ^{13}N to rosette stems in the reproductive stage was not statistically different from the vegetative stage. However, genotype and the transition from vegetative to reproductive stage both had significant effects on ^{13}N partitioning to roots ($P_{genotype}$ = 0.03; $P_{VegStage}$ = 0.01) and flower stalks ($P_{genotype}$ = 0.002; $P_{VegStage}$ < 0.0001). There was a trend for reduced ^{13}N partitioning to roots after the transition to the reproductive stage in all genotypes, and increased ^{13}N partitioning to flower stalks in all but *Atnpf2.12* mutants (Fig. 3). Partitioning of ^{13}N to the flower stalk was 82% lower in *Atnpf2.12* than in the WT (Fig. 3A–B), consistent with the previously reported role of AtNPF2.12 (previously NRT1.6) in early embryo development (Almagro et al., 2008). In addition to reduced ^{13}N partitioning, the *Atnpf2.12* flower stalks were smaller in the ^{13}N experiment, but not significantly different from WT (Table 1).

3.2. High-throughput phenotyping for N-transporter mutants

To further determine the physiological role of the three genes identified above, we conducted a high-throughput phenotyping experiment of the three corresponding *Arabidopsis* mutant lines grown with adequate N and low N availability. Since changes in N status may result in changes in chlorophyll abundance or changes in leaf size (Diaz et al., 2008; Ladha et al., 1998; Neilson et al., 2015), we measured both projected leaf area and relative chlorophyll fluorescence of these mutants using high-throughput imaging.

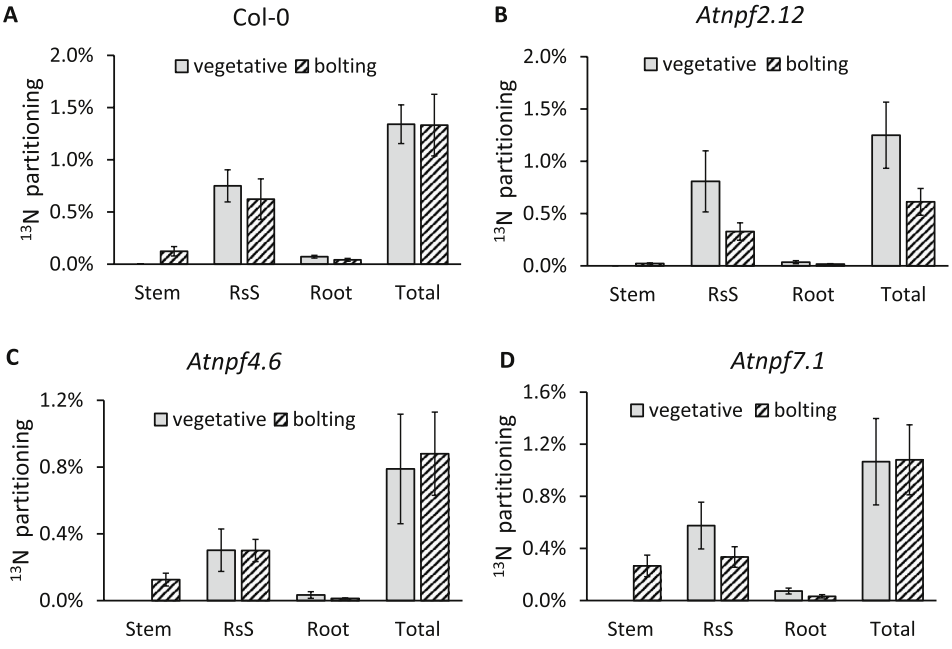

Fig. 3. Partitioning of ^{13}N as a percentage of total ^{13}N in the plant in vegetative- and reproductive-stage *Arabidopsis* plants grown with low N availability. Load leaf ^{13}N (98.5–99.5%) not shown due to scaling. Plants were grouped as either vegetative stage or bolting. Total export included the load leaf petiole (^{13}N presumably in transit), Rosette stems (RsS), root, and flower stalks (stem). **(A)** Col-0. **(B)** *Atnpf2.12*. **(C)** *Atnpf4.6*. **(D)** *Atnpf7.1*. Bars indicate mean ± SEM. Rosette stems, root, and flower stalk data were arcsine transformed for ANOVA to meet the assumption of normality.

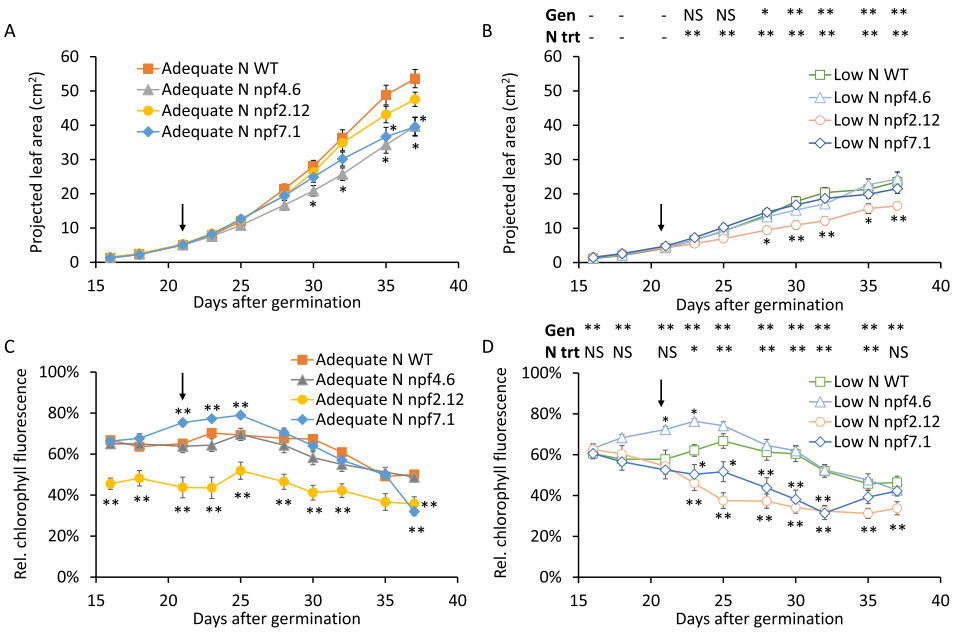

Fig. 4. Rosette growth and chlorophyll fluorescence of WT and *Atnpf* mutants grown with adequate (A & C) or low N (B & D). Total projected leaf area of plants in adequate N treatment **(A)**, and in low N treatment **(B)**. Relative chlorophyll fluorescence, an indicator of tissue N, expressed as proportion of projected leaf area categorized as high or medium chlorophyll fluorescence in plants grown under adequate **(C)** and low **(D)** N conditions. Arrows indicate initiation of flowering. Data are means ± SEM (n = 15). Overall ANOVA P-values for genotype and N treatment effects at each time point are indicated by asterisks above the low N graphs **(C & D)**. Within each N treatment, differences between mutant and WT are indicated by asterisks near those mutant data points that are significantly different from the WT at each time point based on Dunnett's test. Pairwise genotype differences in relative chlorophyll fluorescence in the adequate N treatment were determined using Dunnett's T3 test due to unequal variances (*P < 0.05; **P < 0.01).

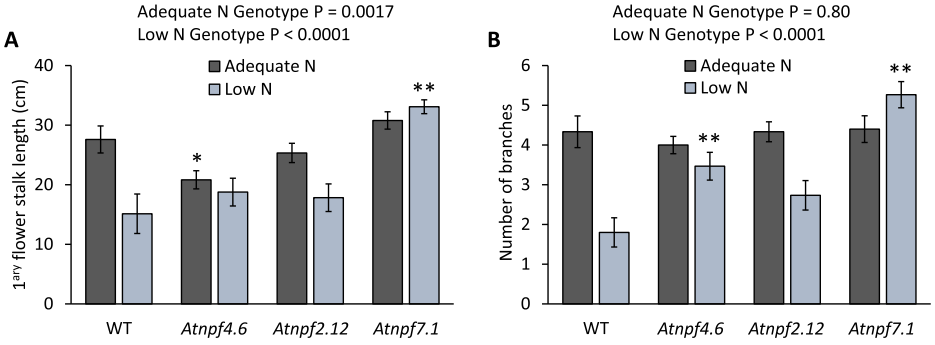

Fig. 5. *Arabidopsis* genotype and N limitation influence flower stalk morphology. Primary flower stalk length **(A)**, and number of flower stalk branches (primary and secondary branches) **(B)** of plants used in the Scanalyzer phenotyping study at the time of final tissue harvest. Bars are means ± SEM (n = 15). P-values are for ANOVA comparing genotypes within each N treatment separately, except for the flower stalk lengths for the low N treatment, which required a Welch's ANOVA due to unequal variances. Asterisks indicate p-values for Dunnett's test comparing mutants with WT within each N treatment, except for stalk lengths in the low N treatment which were compared using Dunnett's T3 test (*P < 0.05; **P < 0.01).

Although low N availability clearly reduced growth of all genotypes, as indicated by projected leaf area (Fig. 4A and B), the plants with low N still survived and produced seeds. The phenotypes of the mutants were subtle. Under adequate N conditions, there was a 25% reduction in projected leaf area at the final measurement date for *Atnpf4.6* and *Atnpf7.1* (Fig. 4A). The reduced growth began much sooner for *Atnpf4.6* than for *Atnpf7.1*. Under low N conditions, only *Atnpf2.12* showed reduced leaf area compared to WT (Fig. 4B). It is interesting that *Atnpf4.6* and *Atnpf7.1* mutants had more branched flower stalks than WT, and in the case of *Atnpf7.1* greater flower stalk length in low N conditions than WT plants (Fig. 5)

In the WT, relative chlorophyll fluorescence decreased late in the reproductive stage (Fig. 4C and D, Supp. Fig. 3), indicating leaf senescence and the associated decline in leaf N at that stage. The decline in chlorophyll content began earlier in the *Atnpf2.12*, *Atnpf4.6,* and *Atnpf7.1* mutants (28 days; 21 days for *Atnpf2.12* in low N) than the WT (32 days) (Fig. 4). The *Atnpf2.12* mutant had moderately low relative chlorophyll fluorescence under both adequate N and low N conditions, while *Atnpf7.*1 had reduced relative chlorophyll fluorescence only under the low N treatment (Fig. 4). Under adequate N, the *Atnpf7.1* mutant had higher relative chlorophyll fluorescence than WT early in the reproductive development, but declined below the WT by the end of the experiment (Fig. 4C). There was a similarly elevated chlorophyll fluorescence in the *Atnpf4.6* mutant, but under low N availability (Fig. 4D). Water content, as indicated by NIR imaging, was similarly high in all plants regardless of genotype and N treatment (Supp. Fig. 4), reflecting that the water supply was not limiting during the experiments.

3.3. *AtNPF7.1 localized in plasma membrane and expressed in pollen*

Since localization of AtNPF4.6 (NRT1.2) and AtNPF2.12 (NRT1.6) have been reported previously (Almagro et al., 2008; Kanno et al., 2012), we determined only the localization of AtNPF7.1 protein. AtNPF7.1 is a putative peptide/nitrate transporter based on sequence similarity (Tsay et al., 2007). Transient expression of *35S:AtNPF7.1:YFP* in *N. benthamiana* leaf epidermis showed that the AtNPF7.1 protein was mainly localized on the plasma membrane (Fig. 6A–D), supporting its role as a putative peptide transporter. The AtNPF7.1:YFP co-localized with the aquaporin-reporter protein, PIP2A:mcherry, which is localized on the plasma membrane (Nelson et al., 2007).

We also fused 2015 bp *AtNPF7.1* promoter region with the GUS reporter gene. In transgenic *Arabidopsis* plants transformed with this *AtNPF7.1*$_{pro}$*:GUS* fusion, the GUS activity was only found in the anthers and pollen (Fig. 6E). Quantitative RT-PCR was conducted for WT roots, young rosette leaves, old rosette leaves, rosette stems, flower stalks, cauline leaves, siliques, and flowers, but *AtNPF7.1* expression was detected only in the flowers (Fig. 6F). This was consistent with the results of an RNA-seq map in which *AtNPF7.1* was expressed in flowers prior to anthesis, and in the anthers after anthesis (Klepikova et al., 2016), and microarray analysis indicating expression of *AtNPF7.1* during pollen development (Honys and Twell, 2004; Winter et al., 2007). Furthermore, growth in low N conditions induced *AtNPF7.1* expression in WT plants (Fig. 6F).

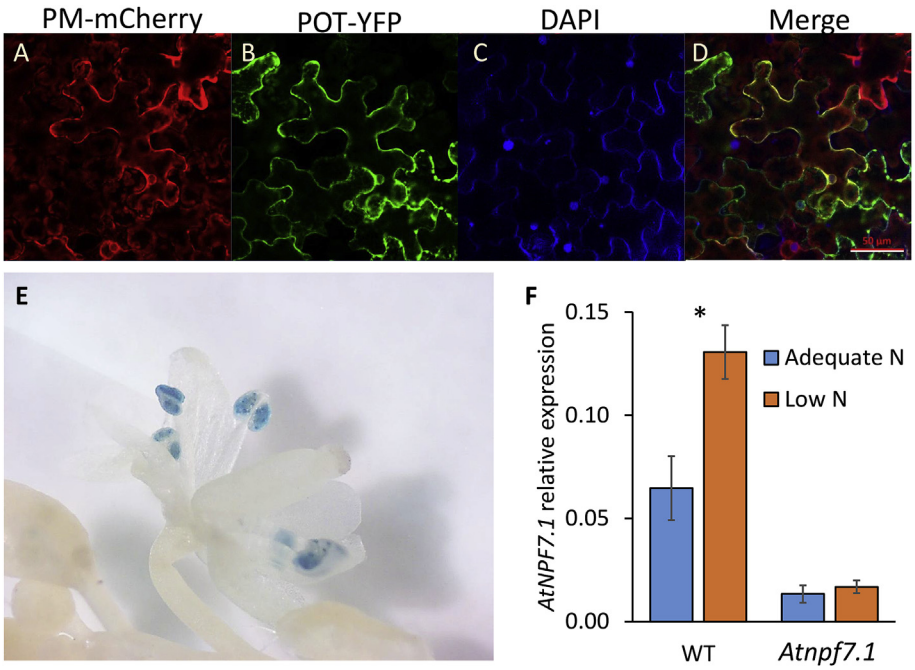

Fig. 6. Expression and localization of *Arabidopsis AtNPF7.1* by transient expression in *N. benthamiana* leaf epidermal cells. Subcellular localization of AtNPF7.1 was on the plasma membrane. Leaves were co-infiltrated with plasma membrane marker-mCherry **(A)**, and *AtNPF7.1-YFP* **(B)**. After imaging mCherry and YFP, leaves were stained with DAPI **(C)**, and the images were merged **(D)**. Scale bar: 50 µm. In transgenic AtNPF7.1$_{Pro}$:GUS *Arabidopsis*, GUS activity was visualized as blue color, which was observed in flowers **(E)**. Image is representative of five independent transgenic lines. Quantitative RT-PCR analysis **(F)** of *AtNPF7.1* gene expression in flower tissues of WT and *Atnpf7.1* mutants grown with adequate or low N. Mean ± SEM, n = 3 (*P < 0.05). (For interpretation of the references to color in this figure legend, the reader is referred to the Web version of this article.)

4. Discussion

Much less is known about the transport of organic nitrogen (N) within the plant, than inorganic N (Tegeder, 2012; Tegeder and Masclaux-Daubresse, 2018). We fed leaves $^{13}NH_3$, which is incorporated into organic forms of N, in order to identify NPFs that influence transport of organic N within *Arabidopsis* plants. As a negative control, we included a mutant of *AtNPF2.13* (*NRT1.7*), which is known to mediate phloem loading of nitrate for transport from leaves to flower stalks (Fan et al., 2009). As expected, the *Atnrt1.7* mutant did not show altered N partitioning compared to WT when fed $^{13}NH_3$, because at cellular pH NH_3 is rapidly non-enzymatically converted to NH_4^+, which is quickly incorporated into organic forms (Hanik et al., 2010). Thus, in addition to identifying three NPF genes that influence remobilization of N from mature leaves in *Arabidopsis*, this study demonstrates the potential power of using $^{13}NH_3$ radiotracer for functional screening assays of organic N export from leaves of a focused set of genetic lines, and the utility of digital imaging to characterize *Arabidopsis* mutants with subtle phenotype differences.

4.1. AtNPF2.12

A previous study of AtNPF2.12 (NRT1.6) revealed its function as a nitrate transporter mainly expressed in the vascular tissue of the silique and funiculus (Almagro et al., 2008). A role for *AtNPF2.12* in nitrate uptake by roots is considered unlikely, since it is not expressed in roots (Almagro et al., 2008). The mutation of *AtNPF2.12* led to abnormal embryos, because not enough nitrate was delivered from maternal tissue to the developing embryo (Almagro et al., 2008). In N starvation conditions, we found the total export of ^{13}N for *Atnpf2.12* mutants was less than WT plants, especially for bolting *Atnpf2.12* plants. In particular, partitioning of ^{13}N to inflorescence stems was substantially reduced (Fig. 3). Thus, AtNPF2.12 appears to alter organic N transport under low N conditions, likely indirectly through its role in nitrate partitioning to seeds. It is possible that AtNPF2.12 may also function in the transport of assimilated organic forms of N. In a previous study, AtNPF2.12 transported nitrate in the oocytes system, but not dipeptides *(Gly-Gly or Leu-Leu)* (Almagro et al., 2008), which reduces the likelihood that AtNPF2.12 transports organic N, but we cannot rule out that AtNPF2.12 might transport other forms of organic N. Many NPF genes transport organic N in addition to, or instead of, nitrate (Corratgé-Faillie and Lacombe, 2017; Tsay et al., 2007). However, the fact that AtNPF2.12 is mainly expressed in the reproductive tissues (Almagro et al., 2008), and yet N partitioning to rosette stems and roots was also reduced suggests that AtNPF2.12 might affect organic N transport indirectly through its effects on nitrate import to developing embryos, perhaps by reducing seed sink strength or by influencing sink-source signaling.

The *Atnpf2.12* mutant plants were significantly smaller than WT plants when N availability was low. It is not clear whether reduced N export caused the reduced growth, or the reduced growth caused reduced N sink strength and lower leaf N export. However, the *Atnpf2.12* mutants had significantly lower N export from leaves on a sink tissue mass basis, indicating that sink strength per unit mass was decreased. This suggests that AtNPF2.12 may be involved in N source-sink interactions during vegetative development, not only during reproduction. Although the strongest expression of AtNPF2.12 is in the developing seeds, there is evidence of moderate expression in leaves, including mesophyll cells (Winter et al., 2007), but *AtNPF2.12* is not expressed in roots (Almagro et al., 2008). Furthermore, chlorophyll content was low in *Atnpf2.12* mutants in both adequate N and low N conditions throughout most of development, suggesting that AtNPF2.12 directly or indirectly affects N utilization within leaves. Reduced chlorophyll may have affected the photosynthetic capacity of the plants, which could affect growth.

4.2. AtNPF4.6

AtNPF4.6 (NRT1.2) was initially identified as a nitrate transporter mainly expressed in the root system (Huang et al., 1999), but was later characterized as an ABA transporter *(AIT1)*, expressed in imbibed seeds, in guard cells, and in vascular tissues in cotyledons, true leaves, hypocotyls, roots, and inflorescence stems (Kanno et al., 2012). The AtNPF4.6 transporter may have dual functions, including a role in nitrate transport, but ABA is the preferred substrate of *Arabidopsis* AtNPF4.6/NRT1.2/AIT1, and nitrate does not competitively inhibit ABA transport by AtNPF4.6 (Kanno et al., 2013). Furthermore, *AtNPF4.6* expression influences plant sensitivity to ABA through its role in ABA transport, but is not otherwise involved in the ABA signaling cascade (Kanno et al., 2012, 2013). Although AtNPF4.6 is expressed in

vascular tissue, it appears to function in localized within-organ transport, rather than vascular loading or unloading (Kanno et al., 2012). In our study, *Atnpf4.6* mutants exported less N to the rosette stem and roots than WT plants under the N starvation condition, which could suggest the possibility of additional roles of AtNPF4.6 in N remobilization and redistribution. Although AtNPF4.6 does not transport histidine, Ala-His$^+$, Ala-Asp$^-$, Ala-Leu (Huang et al., 1999), we cannot rule out the possibility that AtNPF4.6 could play a role in transporting other forms of organic N from the leaf to the sink tissue.

Since ABA promotes leaf senescence (Gao et al., 2016; Lin et al., 2016; Wojciechowska et al., 2018) and N remobilization (El Mannai et al., 2017; Han et al., 2017; Poret et al., 2017), it is also possible that AtNPF4.6 influences organic N export from leaves via its role in ABA signaling. There is previous evidence of antagonistic crosstalk between ABA and nitrate signaling (Alboresi et al., 2005; Matakiadis et al., 2009). *Arabidopsis* knockout mutants of AtNPF4.6 had reduced sensitivity to ABA (Kanno et al., 2012). Three observations suggest that the N sensing pathways in *Atnpf4.6* mutant plants overestimate plant N content: under low N, *Atnpf4.6* mutants exhibited (1) high chlorophyll early in development, (2) reduced N export from mature leaves, and (3) greater flower stalk branching. Previous reports showed that nitrate interferes with ABA signaling by stimulating ABA catabolism (Alboresi et al., 2005; Matakiadis et al., 2009). In turn, the results of our study suggest that reduced ABA sensing in *Atnpf4.6* mutants may have increased the sensitivity of N sensing. It is not clear why rosette and flower stalk growth of *Atnpf4.6* mutants were reduced compared to WT plants in adequate N conditions, but it could have been the result of altered ABA signaling. Expression of AtNPF4.6/AIT1 in *Arabidopsis* leaves and flower stalks alters stomatal conductance (Kanno et al., 2012), which could impact CO_2 availability for photosynthesis and could possibly influence nutrient uptake by altering water flux through the xylem. Alternatively, it is possible that *AtNPF4.6* could influence organic N transport indirectly by altering nitrate uptake by roots, or by altering nitrate partitioning within the plant.

4.3. AtNPF7.1

We identified a previously uncharacterized N cycling-related gene, *AtNPF7.1*, via an *Atnpf7.1* mutant that has reduced organic N export from leaves specifically when N availability was low. Furthermore, *AtNPF7.1* expression was upregulated by low N availability, suggesting a role in N-stress response. However, *AtNPF7.1* was not expressed in roots, suggesting that it does not contribute directly to nitrate uptake from soil. We observed that AtNPF7.1 was localized in the plasma membrane, similar to many other characterized NPF transporters (Almagro et al., 2008; Hu et al., 2014; Kanno et al., 2012; Kiba et al., 2012; Lezhneva et al., 2014; Li et al., 2010; Lin et al., 2008), and was mainly expressed in the flowers, consistent with a previous report (Tsay et al., 2007), particularly in the anthers and pollen. However, the reduction of export from *Atnpf7.1* leaves during both the vegetative and reproductive stages indicates that *AtNPF7.1* must be expressed in some vegetative tissue, possibly at a low level since we did not detect it. In one previous study *AtNPF7.1* expression was not detected in leaves, but in other studies was detected at low levels in mesophyll cells, at higher levels early in guard cell development, at a low level in rosettes, and was upregulated following wounding (Kilian et al., 2007; Klepikova et al., 2016; Winter et al., 2007; Yang et al., 2008). It is not clear whether AtNPF7.1 is involved directly in organic N transport, or if it affects organic N transport indirectly. *AtNPF7.1* is most closely related to *AtNRT1.5*, which loads nitrate into the xylem in roots (Lin et al., 2008). However, since other NPF transporters have been found to transport organic forms of N in addition to nitrate (Corratgé-Faillie and Lacombe, 2017; Tsay et al., 2007), and since AtNPF7.1 is a putative peptide transporter (Tsay et al., 2007), we cannot rule out the possibility that AtNPF7.1 might directly mediate organic N transport. The expression pattern suggests that the major *in vivo* function of AtNPF7.1 may be a role in the delivery of organic N to developing pollen grains.

There are several possible explanations for the observed phenotypes of *Atnpf7.1* mutants in N-stress conditions, which included substantially reduced chlorophyll fluorescence, and flower stalk length and branching similar to or greater than plants grown with adequate soil N. In the first scenario, AtNPF7.1 in WT plants is involved in N delivery to developing anthers and pollen, and the effects of knocking out *AtNPF7.1* on phenotype are passive influences on sink-sink competition for limited N. When *AtNPF7.1* expression increases in WT plants due to N limitation, anthers and pollen would become stronger sinks for N, making proportionally less N available for stalk growth and branch initiation. Knockout of *AtNPF7.1* in the mutant would reduce N uptake by anthers and pollen, increasing the N available for stalk elongation and branch initiation. Changes in the allocation of finite resources from source tissues or amongst multiple sinks can be driven entirely by changes in resource demand by one sink (Minchin et al., 1993). The reduced leaf N export that we observed would indicate that enhanced growth of inflorescence structures in *Atnpf7.1* mutants still did not demand as much N as development of anthers and pollen in WT plants. However, this scenario fails to explain the reduced relative chlorophyll fluorescence in *Atnpf7.1* mutants under low N for most of the reproductive stage.

An alternative scenario is that AtNPF7.1 is involved in N sensing, and the effects of *AtNPF7.1* knockout on phenotype are due to altered sensitivity to N status. Whereas low N availability resulted in WT plants with greatly reduced flower stalk size and complexity, *Atnpf7.1* mutant plants maintained or slightly increased their size and number of branches when N availability was low (Fig. 5). This could result from insensitivity of the *Atnpf7.1* mutant to low N stress, or overestimating the internal abundance of N. Control of branching is under complex regulation by multiple hormones, as well as carbohydrate status (Domagalska and Leyser, 2011; Dun et al., 2012; Gomez-Roldan et al., 2008; Mason et al., 2014). Given the interactions between C and N, it is not surprising that N status can influence inflorescence branching, as seen when N fertilizer is provided to rice (Ding et al., 2014). In *Arabidopsis*, loss of function of a senescence-associated protease that affects N cycling, results in altered inflorescence branching (Guiamét et al., 2014). Since N recycling tends to be more efficient under low N availability (Small, 1972), it would be expected that the *Atnpf7.1* mutant plants may export less N from leaves if they do not perceive N stress or if they overestimate N status. Neither insensitivity to N stress or overestimating plant N status would be expected to result in reduced chlorophyll fluorescence, though.

A third scenario is that AtNPF7.1 is involved in both N delivery to anthers/pollen and N sensing, and that stalk growth and rosette chlorophyll fluorescence are impacted by *AtNPF7.1* knockout through different mechanisms. Reduced N uptake by anthers would make more N available for development of the larger inflorescence stalk and branch structures observed in *Atnpf7.1* mutants. On the other hand, the inability of anthers and/or pollen to take up enough N could trigger a signaling cascade indicating low N status, which could be communicated from sink to source. Signals indicating N starvation may enhance or accelerate senescence processes in leaves in an attempt to fulfill the perceived need for greater N delivery. Normally we would expect N starvation to result in greater N export from leaves. However, even though N demand signals may be sent to leaves from anthers, the actual N uptake into sinks is reduced, which could result in a backup of N transport. Thus, we propose that AtNPF7.1 could influence leaf N export and inflorescence branching through a direct role in nitrate or organic N delivery to anthers and pollen, while influencing leaf chlorophyll degradation through a direct or indirect role in N sensing in floral tissues, which is in turn signaled to source leaves accelerating senescence.

5. Conclusions

We found three mutants with reduced organic N export from leaves under low N conditions. Remobilization of N from older shaded leaves to younger leaves that potentially receive more direct sunlight can be an adaptive response to low N stress. Normal expression of each of these three *AtNPF* genes was required to maintain normal N export during low N availability. One of these genes was previously known to be involved in ABA signaling. Our results suggest that the other two AtNPFs may act in part via signaling, as well. Several other NPFs (NRT1/PTR family) are involved in transporting signaling molecules, in addition to nitrate (Corratgé-Faillie and Lacombe, 2017; Tsay et al., 2007). Most notoriously, AtNRT1.1 links N sensing with auxin transport to influence root development and ultimately root architecture (Krouk et al., 2010; Mounier et al., 2014). Furthermore, although AtNPF2.12 was previously characterized and implicated in nitrate transport into developing embryos (Almagro et al., 2008), the influence of AtNPF2.12 on transport of organic N is a novel finding of our work. The present study adds to the list of known components of N sensing pathways in plants. Future studies should aim to understand how these components interact and function as an integrated system.

Contributions

Fei Gao did most of the molecular work, and all of the localization studies. Abhijit Karve contributed to early molecular work and genotype selection. In consultation with Ben Babst, Michael Schueller designed and built the $^{13}NH_3$ gas delivery system and cuvettes for ^{13}N experiments. Fei Gao conducted the ^{13}N experiments, with some assistance from Ben Babst and Michael Schueller. Ben Babst, Fei Gao, and Lucia Acosta-Gamboa developed the growth protocol to achieve low soil N availability. Lucia Acosta-Gamboa conducted the high throughput phenotyping experiment. Ben Babst and Fei Gao drafted the manuscript. Argelia Lorence supervised the high throughput phenotyping experiment, and edited the manuscript.

Declarations of interest

None.

Acknowledgements

This research was funded by a Plant Imaging Consortium, AR, United States seed grant funded by the AR/MO NSF EPSCoR Track 2 award # IIA-1430427 and IIA-1430428 (to BAB and FG), the USDA National Institute of Food and Agriculture, McIntire-Stennis Program, United States project number 1009319 (to BAB), a Laboratory Directed Research and Development grant from Brookhaven National Laboratory, United States (to BB), by Brookhaven Science Associates, LLC under contract number DE-AC02-98CH10886 with the U.S. Department of Energy, United States, and AL thanks support for the Phenomics Center from the Arkansas Biosciences Institute, United States.

Appendix A. Supplementary data

Supplementary data to this article can be found online at https://doi.org/10.1016/j.plaphy.2019.08.014.

References

Acosta-Gamboa, L.M., Liu, S., Langley, E., Campbell, Z., Castro-Guerrero, N., Mendoza-Cozatl, D., Lorence, A., 2016. Moderate to severe water limitation differentially affects the phenome and ionome of *Arabidopsis*. Funct. Plant Biol. 44, 94–106.

Alboresi, A., Gestin, C., Leydecker, M.-T., Bedu, M., Meyer, C., Truong, H.-N., 2005. Nitrate, a signal relieving seed dormancy in *Arabidopsis*. Plant Cell Environ. 28, 500–512.

Almagro, A., Lin, S.H., Tsay, Y.F., 2008. Characterization of the *Arabidopsis* nitrate transporter NRT1.6 reveals a role of nitrate in early embryo development. Plant Cell 20, 3289–3299.

Babst, B.A., Coleman, G.D., 2018. Seasonal nitrogen cycling in temperate trees: transport and regulatory mechanisms are key missing links. Plant Sci. 270, 268–277.

Breeze, E., Harrison, E., McHattie, S., Hughes, L., Hickman, R., Hill, C., Kiddle, S., Kim, Y.S., Penfold, C.A., Jenkins, D., et al., 2011. High-resolution temporal profiling of transcripts during *Arabidopsis* leaf senescence reveals a distinct chronology of processes and regulation. Plant Cell 23, 873–894.

Clough, S., Bent, A., 1998. Floral dip: a simplified method for *Agrobacterium*-mediated transformation of *Arabidopsis thaliana*. Plant J. 16, 735–743.

Corratgé-Faillie, C., Lacombe, B., 2017. Substrate (un)specificity of *Arabidopsis* NRT1/PTR FAMILY (NPF) proteins. J. Exp. Bot. 68, 3107–3113.

Diaz, C., Lemaıtre, T., Christ, A., Azzopardi, M., Kato, Y., Sato, F., Morot-Gaudry, J.-F., Le Dily, F., Masclaux-Daubresse, C., 2008. Nitrogen recycling and remobilization are differentially controlled by leaf senescence and development stage in *Arabidopsis* under low nitrogen nutrition. Plant Physiol. 147, 1437–1449.

Ding, C., You, J., Chen, L., Wang, S., Ding, Y., 2014. Nitrogen fertilizer increases spikelet number per panicle by enhancing cytokinin synthesis in rice. Plant Cell Rep. 33, 363–371.

Domagalska, M.A., Leyser, O., 2011. Signal integration in the control of shoot branching. Nat. Rev. Mol. Cell Biol. 12, 211–221.

Dun, E.A., de Saint Germain, A., Rameau, C., Beveridge, C.A., 2012. Antagonistic action of strigolactone and cytokinin in bud outgrowth control. Plant Physiol. 158, 487–498.

Dunnett, C.W., 1980. Pairwise multiple comparisons in the unequal variance case. J. Am. Stat. Assoc. 75, 796–800.

El Mannai, Y., Akabane, K., Hiratsu, K., Satoh-Nagasawa, N., Wabiko, H., 2017. The NAC transcription factor gene OsY37 (ONAC011) promotes leaf senescence and accelerates heading time in rice. Int. J. Mol. Sci. 18.

Fan, S.-C., Lin, C.-S., Hsu, P.-K., Lin, S.-H., Tsay, Y.-F., 2009. The *Arabidopsis* nitrate transporter NRT1.7, expressed in phloem, is responsible for source-to-sink remobilization of nitrate. Plant Cell 21, 2750–2761.

Ferrieri, A.P., Agtuca, B., Appel, H.M., Ferrieri, R.A., Schultz, J.C., 2013. Temporal changes in allocation and partitioning of new carbon as ^{11}C elicited by simulated herbivory suggest that roots shape aboveground responses in *Arabidopsis thaliana*. Plant Physiol. 161, 692–704.

Ferrieri, R.A., Herman, E., Babst, B.A., Schueller, M.J., 2018. Managing the soil nitrogen cycle in agroecosytems. In: Lal, R., Stewart, B.A. (Eds.), Advances in Soil Science: Soil Nitrogen Uses and Environmental Impacts. CRC Press, Boca Raton, FL, pp. 343–360.

Ferrieri, R.A., Wolf, A.P., 1983. The chemistry of positron emitting nucleogenic atoms with regard to preparation of labeled compounds of practical utility. Radiochim. Acta 34, 69–83.

Gao, S., Gao, J., Zhu, X., Song, Y., Li, Z., Ren, G., Zhou, X., Kuai, B., 2016. ABF2, ABF3, and ABF4 promote ABA-mediated chlorophyll degradation and leaf senescence by transcriptional activation of chlorophyll catabolic genes and senescence-associated genes in *Arabidopsis*. Mol. Plant 9, 1272–1285.

Gomez-Roldan, V., Fermas, S., Brewer, P.B., Puech-Pages, V., Dun, E.A., Pillot, J.-P., Letisse, F., Matusova, R., Danoun, S., Portais, J.-C., et al., 2008. Strigolactone inhibition of shoot branching. Nature 455, 189–194.

Gomez, S., Ferrieri, R.A., Schueller, M.J., Orians, C.M., 2010. Methyl jasmonate elicits rapid changes in carbon and nitrogen dynamics in tomato. New Phytol. 188, 835–844.

Guiamét, J.J., Borniego, M.L., Martinez, D.E., Tyystjärvi, E., Aro, E.-M., Battchikova, N., 2014. SASP, a Senescence-Associated Subtilisin Protease, is involved in reproductive development and determination of silique number in *Arabidopsis*. J. Exp. Bot. 66, 161–174.

Han, Y.-L., Liao, J.-Y., Yu, Y., Song, H.-X., Rong, N., Guan, C.-Y., Lepo, J.E., Ismail, A.M., Zhang, Z.-H., 2017. Exogenous abscisic acid promotes the nitrogen use efficiency of *Brassica napus* by increasing nitrogen remobilization in the leaves. J. Plant Nutr. 40, 2540–2549.

Hanik, N., Gomez, S., Schueller, M.J., Orians, C.M., Ferrieri, R.A., 2010. Use of gaseous $^{13}NH_3$ administered to intact leaves of *Nicotiana tabacum* to study changes in nitrogen utilization during defense induction. Plant Cell Environ. 33, 2173–2179.

Havé, M., Marmagne, A., Chardon, F., Masclaux-Daubresse, C., 2017. Nitrogen remobilization during leaf senescence: lessons from *Arabidopsis* to crops. J. Exp. Bot. 68, 2513–2529.

He, F., Karve, A.A., Maslov, S., Babst, B.A., 2016. Large-scale public transcriptomic data mining reveals a tight connection between the transport of nitrogen and other transport processes in *Arabidopsis*. Front. Plant Sci. 7, 1207 doi: 1210.3389/fpls.2016.01207.

Honys, D., Twell, D., 2004. Transcriptome analysis of haploid male gametophyte development in *Arabidopsis*. Genome Biol. 5, R85.

Hu, Y., Fernández, V., Ma, L., 2014. Nitrate transporters in leaves and their potential roles in foliar uptake of nitrogen dioxide. Front. Plant Sci. 5, 360.

Huang, N.-C., Liu, K.-H., Lo, H.-J., Tsay, Y.-F., 1999. Cloning and functional characterization of an *Arabidopsis* nitrate transporter gene that encodes a constitutive component of low-affinity uptake. Plant Cell 11, 1381–1392.

Jefferson, R.A., Kavanagh, T.A., Bevan, M.W., 1987. GUS fusions: beta-glucuronidase as a sensitive and versatile gene fusion marker in higher plants. EMBO J. 6, 3901–3907.

Kanno, Y., Hanada, A., Chiba, Y., Ichikawa, T., Nakazawa, M., Matsui, M., Koshiba, T., Kamiya, Y., Seo, M., 2012. Identification of an abscisic acid transporter by functional screening using the receptor complex as a sensor. Proc. Natl. Acad. Sci. U.S.A. 109, 9653–9658.

Kanno, Y., Kamiya, Y., Seo, M., 2013. Nitrate does not compete with abscisic acid as a substrate of AtNPF4.6/NRT1.2/AIT1 in *Arabidopsis*. Plant Signal. Behav. 8, e26624.

Kiba, T., Feria-Bourrellier, A.-B., Lafouge, F., Lezhneva, L., Boutet-Mercey, S., Orsel, M.,

Brehaut, V., Miller, A., Daniel-Vedele, F., Sakakibara, H., et al., 2012. The *Arabidopsis* nitrate transporter NRT2.4 plays a double role in roots and shoots of nitrogen-starved plants. Plant Cell 24, 245–258.
Kilian, J., Whitehead, D., Horak, J., Wanke, D., Weinl, S., Batistic, O., D'Angelo, C., Bornberg-Bauer, E., Kudla, J., Harter, K., 2007. The AtGenExpress global stress expression data set: protocols, evaluation and model data analysis of UV-B light, drought and cold stress responses. Plant J. 50, 347–363.
Klepikova, A.V., Kasianov, A.S., Gerasimov, E.S., Logacheva, M.D., Penin, A.A., 2016. A high resolution map of the *Arabidopsis thaliana* developmental transcriptome based on RNA-seq profiling. Plant J. 88, 1058–1070.
Krouk, G., Lacombe, B., Bielach, A., Perrine-Walker, F., Malinska, K., Mounier, E., Hoyerova, K., Tillard, P., Leon, S., Ljung, K., et al., 2010. Nitrate-regulated auxin transport by NRT1.1 defines a mechanism for nutrient sensing in plants. Dev. Cell 18, 927–937.
Ladha, J.K., Tirol-Padre, A., Punzalan, G.C., Castillo, E., Singh, U., Reddy, C.K., 1998. Nondestructive estimation of shoot nitrogen in different rice genotypes. Agron. J. 90, 33–40.
Léran, S., Varala, K., Boyer, J.-C., Chiurazzi, M., Crawford, N., Daniel-Vedele, F., David, L., Dickstein, R., Fernandez, E., Forde, B., et al., 2014. A unified nomenclature of NITRATE TRANSPORTER 1/PEPTIDE TRANSPORTER family members in plants. Trends Plant Sci. 19, 5–9.
Lezhneva, L., Kiba, T., Feria-Bourrellier, A.-B., Lafouge, F., Boutet-Mercey, S., Zoufan, P., Sakakibara, H., Daniel-Vedele, F., Krapp, A., 2014. The *Arabidopsis* nitrate transporter NRT2.5 plays a role in nitrate acquisition and remobilization in nitrogen-starved plants. Plant J. 80, 230–241.
Li, J.-Y., Fu, Y.-L., Pike, S.M., Bao, J., Tian, W., Zhang, Y., Chen, C.-Z., Zhang, Y., Li, H.-M., Huang, J., et al., 2010. The *Arabidopsis* nitrate transporter NRT1.8 functions in nitrate removal from the xylem sap and mediates cadmium tolerance. Plant Cell 22, 1633–1646.
Lin, S.-H., Kuo, H.-F., Canivenc, G., Lin, C.-S., Lepetit, M., Hsu, P.-K., Tillard, P., Lin, H.-L., Wang, Y.-Y., Tsai, C.-B., et al., 2008. Mutation of the *Arabidopsis* NRT1.5 nitrate transporter causes defective root-to-shoot nitrate transport. Plant Cell 20, 2514–2528.
Lin, X., Wang, D., Gu, S.B., White, P.J., Han, K., Zhou, J., Jin, S.P., 2016. Effect of supplemental irrigation on the relationships between leaf ABA concentrations, tiller development and photosynthate accumulation and remobilization in winter wheat. Plant Growth Regul. 79, 331–343.
Mason, M.G., Ross, J.J., Babst, B.A., Wienclaw, B.N., Beveridge, C.A., 2014. Sugar demand, not auxin, is the initial regulator of apical dominance. Proc. Natl. Acad. Sci. U.S.A. 111, 6092–6097.
Matakiadis, T., Alboresi, A., Jikumaru, Y., Tatematsu, K., Pichon, O., Renou, J.-P., Kamiya, Y., Nambara, E., Truong, H.-N., 2009. The *Arabidopsis* abscisic acid catabolic gene *CYP707A2* plays a key role in nitrate control of seed dormancy. Plant Physiol. 149, 949–960.
McDonald, J.H., 2014. Handbook of Biological Statistics, third ed. Sparky House Publishing, Baltimore, Maryland.
Minchin, P.E.H., Thorpe, M.R., Farrar, J., 1993. A simple mechanistic model of phloem transport which explains sink priority. J. Exp. Bot. 44, 947–955.
Mounier, E., Pervent, M., Ljung, K., Gojon, A., Nacry, P., 2014. Auxin-mediated nitrate signalling by NRT1.1 participates in the adaptive response of *Arabidopsis* root architecture to the spatial heterogeneity of nitrate availability. Plant Cell Environ. 37, 162–174.
Murashige, T., Skoog, F., 1962. A revised medium for rapid growth and bio assays with tobacco tissue cultures. Physiol. Plant. 15, 473–497.
Neilson, E.H., Edwards, A.M., Blomstedt, C.K., Berger, B., Møller, B.L., Gleadow, R.M., 2015. Utilization of a high-throughput shoot imaging system to examine the dynamic phenotypic responses of a C4 cereal crop plant to nitrogen and water deficiency over time. J. Exp. Bot. 66, 1817–1832.
Nelson, B.K., Cai, X., Nebenführ, A., 2007. A multicolored set of *in vivo* organelle markers for co-localization studies in *Arabidopsis* and other plants. Plant J. 51, 1126–1136.
Pankievicz, V.C.S., do Amaral, F.P., Santos, K.F.D.N., Agtuca, B., Xu, Y., Schueller, M.J., Arisi, A.C.M., Steffens, M.B.R., de Souza, E.M., Pedrosa, F.O., et al., 2015. Robust biological nitrogen fixation in a model grass–bacterial association. Plant J. 81, 907–919.
Poret, M., Chandrasekar, B., van der Hoorn, R., Coquet, L., Jouenne, T., Avice, J.-C., 2017. Proteomic investigations of proteases involved in cotyledon senescence: a model to explore the genotypic variability of proteolysis machinery associated with nitrogen remobilization efficiency during the leaf senescence of oilseed rape. Proteomes 5, 29.
Santiago, J.P., Tegeder, M., 2016. Connecting source with sink: the role of *Arabidopsis* AAP8 in phloem loading of amino acids. Plant Physiol. 171, 508–521.
Schmid, M., Davison, T.S., Henz, S.R., Pape, U.J., Demar, M., Vingron, M., Schölkopf, B., Weigel, D., Lohmann, J.U., 2005. A gene expression map of *Arabidopsis thaliana* development. Nat. Genet. 37, 501–506.
Small, E., 1972. Photosynthetic rates in relation to nitrogen recycling as an adaptation to nutrient deficiency in peat bog plants. Can. J. Bot. 50, 2227–2233.
Straatman, M.G., 1977. A look at ^{13}N and ^{15}O in radiopharmaceuticals. Int. J. Appl. Radiat. Isot. 28, 13–20.
Taylor, L., Nunes-Nesi, A., Parsley, K., Leiss, A., Leach, G., Coates, S., Wingler, A., Fernie, A.R., Hibberd, J.M., 2010. Cytosolic pyruvate,orthophosphate dikinase functions in nitrogen remobilization during leaf senescence and limits individual seed growth and nitrogen content. Plant J. 62, 641–652.
Tegeder, M., 2012. Transporters for amino acids in plant cells: some functions and many unknowns. Curr. Opin. Plant Biol. 15, 315–321.
Tegeder, M., Masclaux-Daubresse, C., 2018. Source and sink mechanisms of nitrogen transport and use. New Phytol. 217, 35–53.
Tsay, Y.-F., Chiu, C.-C., Tsai, C.-B., Ho, C.-H., Hsu, P.-K., 2007. Nitrate transporters and peptide transporters. FEBS Lett. 581, 2290–2300.
Winter, D., Vinegar, B., Nahal, H., Ammar, R., Wilson, G.V., Provart, N.J., 2007. An "electronic fluorescent pictograph" browser for exploring and analyzing large-scale biological data sets. PLoS One 2, e718.
Wojciechowska, N., Sobieszczuk-Nowicka, E., Bagniewska-Zadworna, A., 2018. Plant organ senescence – regulation by manifold pathways. Plant Biol. 20, 167–181.
Yang, Y., Costa, A., Leonhardt, N., Siegel, R.S., Schroeder, J.I., 2008. Isolation of a strong *Arabidopsis* guard cell promoter and its potential as a research tool. Plant Methods 4, 6.
Zhang, L., Tan, Q., Lee, R., Trethewy, A., Lee, Y.-H., Tegeder, M., 2010. Altered xylem-phloem transfer of amino acids affects metabolism and leads to increased seed yield and oil content in *Arabidopsis*. Plant Cell 22, 3603–3620.